

# Molecular Hydrogen Suppresses Reactive Astrogliosis Related to Oxidative Injury during Spinal Cord Injury in Rats

Fang-Ting Liu,<sup>1</sup> Sheng-Ming Xu,<sup>2</sup> Zheng-Hua Xiang,<sup>3</sup> Xiang-Nan Li,<sup>1</sup> Jian Li,<sup>1</sup> Hong-Bin Yuan<sup>1</sup> & Xue-Jun Sun<sup>4</sup><sup>1</sup> Department of Anesthesiology, Neuroscience Research Centre, Changzheng Hospital, Second Military Medical University, Shanghai, China<sup>2</sup> Department of Orthopaedics, Changzheng Hospital, Second Military Medical University, Shanghai, China<sup>3</sup> Key Laboratory of Molecular Neurobiology, Department of Neurobiology, Ministry of Education, Second Military Medical University, Shanghai, China<sup>4</sup> Department of Diving Medicine, Second Military Medical University, Shanghai, China

## Keywords

Astrogliosis; Glial scar; Hydrogen; Oxidative injury; Spinal cord injury.

## Correspondence

Hongbin Yuan, Department of Anesthesiology, Neuroscience Research Centre, Changzheng Hospital, Second Military Medical University, Shanghai 200003, China.

Tel./Fax: +(8621)8188-5822;

E-mail: jfjczyy@aliyun.com

and

Xuejun Sun, Department of Diving Medicine, Faculty of Naval Medicine, Second Military Medical University, Shanghai 200433, China.

Tel./Fax: +(8621)6549-2382;

E-mail: sunxjk@hotmail.com

Received 25 November 2013; revision 28

February 2014; accepted 2 March 2014

## SUMMARY

**Aims:** Spinal cord injury (SCI) can induce excessive astrocyte activation. Hydrogen has been deemed as a novel antioxidant. We investigated whether molecular hydrogen could act as an antiastrogliosis agent during SCI and oxidative injury in experimental rats and cultured astrocytes. **Methods:** Hydrogen-rich saline (HS, 8 mL/kg, i.p.) was injected every 12 h after SCI in rats. The expression of STAT3, p-STAT3, and glial fibrillary acidic protein (GFAP); the release of IL-1 $\beta$ , IL-6, and TNF- $\alpha$ ; and astrogliosis, along with the BBB score, were evaluated. Culturing astrocytes with hydrogen-rich medium, the intracellular reactive oxygen species (ROS), astrogliosis, and the release of proinflammatory cytokines were assessed after H<sub>2</sub>O<sub>2</sub>-induced injury. **Results:** In the HS group, the expression of STAT3, p-STAT3, and GFAP and the proinflammatory cytokines were decreased in local spinal cord on postoperation day (POD) 3; on PODs 7 and 14, reactive astrogliosis was suppressed, and the locomotor function was also improved. Furthermore, hydrogen-rich medium attenuated the intracellular production of ROS (especially HO $\bullet$ ), astrogliosis, and the secretion of proinflammatory cytokines in astrocytes 12 h after H<sub>2</sub>O<sub>2</sub>-induced injury. **Conclusions:** Molecular hydrogen could suppress reactive astrogliosis after contusive SCI and reduce the release of proinflammatory cytokines produced by active astrocytes related to oxidative injury. Thus, molecular hydrogen is potential to be a neuroprotective agent.

doi: 10.1111/cns.12258

The first two authors contributed equally to this work.

## Introduction

Astrocytes are special glial cells with various important physiological functions and are located throughout the central nervous system (CNS). Nearly all types of CNS injury can result in the activation of astrocytes, which is deemed as a reliable and sensitive pathological hallmark of CNS injury [1]. Primary traumatic spinal cord injury (SCI) induces the release of reactive oxygen species (ROS), such as superoxide anion (O<sub>2</sub><sup>-</sup>), hydrogen peroxide (H<sub>2</sub>O<sub>2</sub>), and hydroxyl radical (HO $\bullet$ ), within several minutes to hours [2,3]. ROS is considered to be a crucial factor related to secondary SCI; it can induce a series of cascade reactions, which not only aggravate the dysfunction or death of neurons but also expand the scope of injury and inflammation [4]. In addition,

ROS can activate astrocytes and is one of the main causes of astrocyte activation [5]. Besides releasing amounts of inflammatory cytokines and aggravating inflammation, astrogliosis leads to excessive secretion of proteoglycans and intermediate filaments, such as glial fibrillary acidic protein (GFAP), which leads to the formation of glial scar, and has been regarded as a critical factor hindering axonal repair and regeneration [6–9]. As GFAP has been recognized as a sensitive and reliable marker for reactive astrogliosis after CNS injury [1], we used it as a target index in our study.

Hydrogen has been proven to be a safe and effective novel antioxidant [10,11]. Hydrogen products have fewer adverse effects than most known antioxidants, because of their ability to penetrate biomembranes and selectively scavenge detrimental

ROS, such as HO• and peroxynitrite (ONOO<sup>-</sup>), without disturbing metabolic oxidation–reduction reactions [10,12,13]. In animal models, inhalation of hydrogen gas or intraperitoneal injection of hydrogen-saturated saline (also called hydrogen-rich saline, HS) can effectively inhibit ischemia–reperfusion-induced oxidative stress in brain, liver, heart, intestine, and other tissues [10,14–16]. Moreover, our preliminary study has demonstrated that, after SCI, intraperitoneal injection of HS can not only decrease the production of ROS and neuronal apoptosis in the spinal cord but also promote recovery of locomotor function [11]. However, it remains unknown whether these protective effects are associated with astrogliosis suppression. In this study, we used a rat contusive SCI model (*in vivo*), and an induced oxidative damage cell model (*in vitro*), to verify that reactive astrogliosis and subsequent glial scar, as well as inflammation expansion induced by SCI, can be suppressed by hydrogen-rich liquid. This study suggests that antiastrogliosis is a potential neuroprotective mechanism of molecular hydrogen.

## Materials and methods

### Preparation of Hydrogen-rich Saline (HS) and Hydrogen-rich Medium (HM)

The methods of producing and storing HS and hydrogen-rich medium (HM) have been previously described [11]. The HS and HM were provided by the Department of Diving Medicine in the Second Military Medical University and produced every week and were stored under atmospheric pressure at 4°C in airtight bags.

### Experimental Animal Models and Experimental Protocols

#### Animals

Adult male Sprague–Dawley rats (200–230 g) were obtained from the Animal Center at the Second Military Medical University, Shanghai, China. All animals were bred with standard laboratory diet and water and housed in a temperature (25°C)- and humidity (60%)-controlled facility under a 12/12-h light/dark cycle. The Animal Care and Use Committee of the Second Military Medical University approved all experimental protocols according to the Health Guide for Care and Use of Laboratory Animals (revised in 1996).

#### Contusive Spinal Cord Injury (SCI)

Spinal cord injury was induced with Allen's impact model as described previously [11,17]. Briefly, after rats were anesthetized with 10% chloral hydrate (0.3 mL/100 g, *i.p.*), a steel rod with a flat tip (2 mm diameter), weighing 10 g, was dropped from a height of 2.5 cm on the exposed region of dura mater at the thoracic (T) 10–11 spinal level. Then, the muscle and skin were sutured, and the wound was disinfected. All instruments were sterilized before the operation. After the surgery, penicillin was injected intramuscularly to each rat for 3 days to prevent infection (20 IU, once a day), and bladder evacuation was performed twice a day.

### Experimental Groups and Treatment

Rats were randomly divided into three groups as follows: (1) sham control group—sham-operated plus normal saline (NS, 0.9% NaCl; *n* = 24), rats of this group had their dura exposed without contusive SCI; (2) Allen + NS group—rats were given Allen's SCI surgery plus NS (*n* = 24); and (3) Allen + HS group—SCI plus HS (*n* = 24). Immediately after the surgery had been accomplished, NS or HS was injected (8 mL/kg, *i.p.*) and then was administered every 12 h until the animals were sacrificed.

### Functional Test

Hind limb neurological function was evaluated before surgery (D 0) and on postoperation days (PODs) 1, 7, and 14 using the Basso, Beattie, and Bresnahan locomotor scale (BBB scale), as previously described [11]. Six rats per group were randomly selected for the functional test. Each rat was placed in an open field and observed for 5 min. Two observers who were blind to the experimental treatments did all the behavioral assessments.

### Immunohistochemistry (IHC)

The activation of astrocytes was examined by measuring the production of GFAP (fluorescence intensity). Briefly, on PODs 7 and 14, six rats per group were sacrificed after the functional test. The rats were deeply anesthetized with 10% chloral hydrate (0.4 mL/100 g, *i.p.*) and transcardially perfused with 50 mL ice-cold NS, followed by 150 mL fixative (4% paraformaldehyde (*w/v*) in 0.1 M phosphate buffer (pH 7.4; 4°C)) over 6 min. Then, spinal cord segments containing the T10 impact epicenter, about 10 mm in length, were dissected from each rat and postfixed with the same fixative fluid overnight (4°C). The samples were transferred to a 20% sucrose buffer overnight and then into 30% sucrose buffer for dehydration and cryoprotection at 4°C overnight. Subsequently, the samples were sagittally sectioned at 20 μm thickness, and the sections of the gray matter were collected in 0.1 M phosphate buffer (PB, pH 7.4); sequentially, one per five sections were selected for observation (the distance between sections is 100 μm). Six sections per sample were blocked in 2% BSA (Sigma, St. Louis, MO, USA) with 0.1% Triton-X 100 (Sigma) for 10 min in a water bath kettle at 95°C, washed three times with 0.1 M PBS (pH 7.4), and then were incubated with rabbit-anti-GFAP primary antibody (1:200; Abcam, Cambridge, MA, USA) diluted in antibody diluent containing 10% normal goat serum for 16 h at 4°C. After rinsing three times, the sections were incubated with TRITC-conjugated goat anti-rabbit secondary antibody (1:200; Jackson Immuno Research, West Grove, PA, USA) for 2 h at room temperature (RT). After rinsing, sections were incubated with 1 μg/mL Hoechst dye in PBS for 10 min at RT. Sections were washed again, mounted on slides, and coverslipped with PBS containing 50% glycerol. Fluorescence was visualized with a Nikon digital camera DXM1200 (Nikon, Tokyo, Japan) adapted to a Nikon Eclipse E600 fluorescence microscope (Nikon). Using Image-Pro 5.0 software, the GFAP fluorescence intensity of each selected image (five epicentral areas per section) was measured and normalized to obtain intensity ratios that were compared between experimental groups.

## Western blot (WB)

On POD 3, six rats per group were sacrificed for examination of STAT3, p-STAT3, and GFAP expression. The rats were also deeply anesthetized (as described previously) and killed by decapitation. Spinal cord segments (as described previously) were dissected from each rat and were then lysed with 20 mM Tris-HCl buffer (pH 8.0; Sigma). The concentration of protein in the homogenate was determined using a BCA reagent (Pierce, Rockford, IL, USA). Protein samples (100 µg) were loaded in each lane, separated by sodium dodecyl sulfate-polyacrylamide gel electrophoresis (SDS-PAGE; 10% polyacrylamide gels), electro-transferred onto nitrocellulose membrane, incubated with a blocking buffer (1 × TBS with 5% w/v fat-free dry milk) for 2 h, and then incubated with rabbit-anti-GFAP primary antibody (1:1,000; Abcam), rabbit-anti-STAT3 primary antibody (1:1,000; Abcam), rabbit-anti-p-STAT3 (phospho-Y705) primary antibody (1:1,000; Abcam), or rabbit-anti-β-actin (1:1000; Abcam) at 4°C overnight. The polyvinylidene difluoride (PVDF) membranes were washed five times with TBST (1 × TBS and 0.1% Tween 20) and then were incubated with phosphatase-conjugated goat anti-rabbit IgG (Beyotime, China) diluted 1:1,000 in 2% BSA in PBS for 1 h at RT. The color development was performed with 400 µg/mL nitro-blue tetrazolium, 200 µg/mL 5-bromo-4-chloro-3-indolyl phosphate, and 100 mg/mL levamisole in TSM2 (0.1 M Tris-HCl buffer, pH 9.5, 0.1 M NaCl, and 0.05 M MgCl<sub>2</sub>) in the dark. Bands were scanned and quantified by a GS-700 Imaging Densitometer with Multi-Analyst 1.1 software (Bio-Rad Laboratories, Richmond, CA, USA).

## Cell Culture and Experimental Protocols

### Astrocyte-purified Cultures

Astrocytes were harvested from neonatal rats (P2-3) as previously described [18]. The mixed cells were plated onto PLL-coated culture flasks and incubated in DMEM (Gibco, Grand Island, NY, USA) containing 10% FBS (Sigma). After 6–10 days (media were changed every 2–3 days), microglia and oligodendrocyte lineage cells were removed by shaking the culture at 2.5 *g* at 37°C in 5% CO<sub>2</sub> overnight. Finally, astrocytes were collected and plated onto coverslips in 12-well plates for analysis. Highly pure astrocyte cultures (>96%) were assessed by immunocytochemical staining with the anti-GFAP antibody (results not shown). Cells were cultured for 24 h before treatment.

### Experimental Groups and Treatment

Pure astrocytes (1 × 10<sup>5</sup>/cm<sup>2</sup>) were divided into four groups: 1) control, cultured with normal medium (NM); 2) HM, cultured with hydrogen-rich medium (HM); 3) NM + H<sub>2</sub>O<sub>2</sub>, cultured with NM containing 100 µM H<sub>2</sub>O<sub>2</sub> (Sigma) and 15 µM FeCl<sub>2</sub> (Sigma); 4) HM + H<sub>2</sub>O<sub>2</sub>, cultured with HM containing 100 µM H<sub>2</sub>O<sub>2</sub> and 15 µM FeCl<sub>2</sub> after pretreatment of HM for 1 h. The oxidative injury of astrocytes was induced by H<sub>2</sub>O<sub>2</sub>, which can not only permeate cell membranes, but also induce remarkable production of HO• with the existence of ferrous ions (called Fenton action). The

respective media were changed every 6 h to maintain the concentration of hydrogen at 0.6 mM [19]. Treatments were carried out for 12 h, and then the supernatant or cells were collected for different assays.

## Assay of Intracellular Reactive Oxygen Species

2', 7'-Dichlorodihydrofluorescein diacetate (DCF) is a fluorogenic dye that measures ROS activity within the cells. Hydroxyphenyl fluorescein (HPF) is a new fluorescein derivative that selectively reacts with the HO•. According to the manufacturer's instructions, after rinsing with D-Hank (Gibco), 10 µM DCF (Beyotime, China) or HPF (Invitrogen, Carlsbad, CA, USA) was added to the cells and then incubated in the dark for 30 min at RT. After rinsing three times with medium without FBS, the cells were viewed with a laser confocal microscope (×400; fluoview 300; Olympus, Japan). The fluorescence was excited at 488 nm, and the emitted light was observed at 515–540 nm. The fluorescence signal was assessed qualitatively and compared between groups.

## Immunocytochemistry (ICC)

Twelve hours after treatments, the astrogliosis was examined by measuring GFAP fluorescence intensity as described previously [18]. Briefly, astrocytes were fixed with 4% paraformaldehyde in PBS for 20 min, washed with 0.1 M PBS (pH 7.4), and then incubated overnight at 4°C with rabbit-anti-GFAP primary antibody (1:200; Abcam). After washing three times with PBS, cells were incubated with TRITC-conjugated goat anti-rabbit secondary antibody (1:200; Jackson Immuno Research) for 90 min at RT and then washed and incubated with 1 µg/mL Hoechst dye in PBS for 10 min at RT. The coverslips were mounted with PBS containing 50% glycerol. Fluorescence visualization and the measure of GFAP fluorescence intensity were the same as described in Immunohistochemistry (IHC).

## DNA Synthesis

DNA synthesis (bromodeoxyuridine incorporation, BrdU) was assayed as previously described to evaluate the proliferation of astrocytes [20]. Briefly, for each group, cells received 10 µM BrdU (Sigma) 10 min before treatments. After 12 h, cells were fixed in 10% neutral buffered formalin for 10 min and stained with anti-BrdU primary antibody (1:100; Abcam). The subsequent steps were the same as GFAP immunocytochemistry. Percentages of stained cells were compared.

## Enzyme-linked Immunosorbent Assay (ELISA)

After experimental treatments, spinal cord sections were pulverized with normal saline and centrifuged at 10,000 *g* for 10 min; the culture medium was collected from each well and centrifuged at 600 *g* for 10 min. The supernatant of each group was collected for IL-1β, IL-6, and TNF-α concentration assays with commercial ELISA kits (R&D Systems, Minneapolis, MN, USA), according to the manufacturers' instructions. The absorbance at 450 nm was read with a Bio-Rad model 680 microplate spectrophotometer (Bio-Rad).

## Statistical Analysis

Each experiment was repeated at least three times independently. Statistical analysis was performed with GraphPad Prism software version 5.0 (GraphPad Software Inc, San Diego, CA, USA). Data were expressed as mean  $\pm$  SEM, and the differences between groups were analyzed by Student's *t*-test and one-way ANOVA. A two-way ANOVA with repeated measures was used to compare matched data at multiple time points.  $P < 0.05$  was considered statistically significant.

## Results

### The Release of Proinflammatory Cytokines was Attenuated by Hydrogen-rich Saline Administration in the Acute Phase of SCI

In the acute phase of SCI, IL-1 $\beta$ , IL-6, and TNF- $\alpha$  are the initial triggers of reactive astrogliosis [8]. Here, the content of IL-1 $\beta$ , IL-6, and TNF- $\alpha$  in local contusive spinal cord was measured by ELISA. On POD 3, the production of these three classical injury-induced proinflammatory cytokines was remarkably increased in the NS group (vs. sham,  $P < 0.01$ ) and was notably attenuated by hydrogen-rich saline administration (vs. NS,  $P < 0.01$ ,  $P < 0.01$ , and  $P < 0.05$ , respectively; Figure 1A).

### Hydrogen-rich Saline Suppressed the Reactive Astrogliosis after SCI

After the experimental contusive spinal cord injury, the production of STAT3, p-STAT3, and GFAP expressed by astrocytes was increased in the NS group (vs. sham,  $P < 0.01$ ) and was reduced by hydrogen-rich saline administrated intraperitoneally on POD 3 (vs. NS,  $P < 0.01$ ,  $P < 0.05$ , and  $P < 0.01$ , respectively; Figure 1B,C). Morphologically, the characteristics of astrogliosis were hypertrophy and hyperplasia, and functionally, the expression of GFAP (measured by the fluorescence intensity) was dramatically augmented on POD 7 (NS vs. sham,  $P < 0.01$ ; Figure 2A,B) and POD 14 (NS vs. sham,  $P < 0.01$ ; Figure 2C,D). Hydrogen-rich saline administration significantly suppressed the astrogliosis and alleviated the excessive expression of GFAP (vs. NS,  $P < 0.05$  and  $P < 0.01$ , respectively; Figure 2). In particular, the GFAP intensity decreased 65.7% on POD 14 more than 18.2% on POD 7 ( $P < 0.01$ ), which means that the astrogliosis was suppressed more significantly on POD 14, although it was slightly significant on POD 7.

### Hydrogen-rich Saline Promoted the Recovery of Hind Limb Locomotor Function after SCI

Spinal cord injury severely affected the locomotor function. The BBB score of all rats in NS and HS groups extremely decreased on POD 1, but rats of the HS group exhibited higher BBB scores on PODs 7 and 14 (HS vs. NS,  $P < 0.01$ ). This indicated significantly improved locomotor function. In addition, a two-way ANOVA with repeated measures showed a treatment effect of HS over time ( $P < 0.01$ ; Figure 3).

### Hydrogen-rich Medium Reduced the H<sub>2</sub>O<sub>2</sub>-induced Intracellular Production of ROS in Purified Astrocytes

Twelve hours after treatments, each group of astrocytes was prepared for intracellular ROS assays. There was no difference between control and single HM groups, but the total amount of ROS (Figure 4A,B, assayed by DCF intensity) and especially HO $\bullet$  (Figure 4C,D, selectively assayed by HPF intensity) was distinctly increased by adding H<sub>2</sub>O<sub>2</sub> (vs. control,  $P < 0.01$ , both). However, the synthesis of intracellular ROS and especially HO $\bullet$  was significantly decreased by HM (vs. NM + H<sub>2</sub>O<sub>2</sub>,  $P < 0.01$ , both; Figure 4).

### The Hypertrophy and Proliferation of Astrocytes Induced by Oxidant Injury were Inhibited by Hydrogen-rich Medium

Through GFAP staining, the morphological characteristic of hypertrophy attributed to astrogliosis was obviously observed 12 h after H<sub>2</sub>O<sub>2</sub>-induced oxidant injury and was notably inhibited by HM (Figure 5A). To observe oxidant-induced proliferation of astrocytes from the DNA level, we labeled cells with BrdU. The percentage of positive cells was significantly increased by H<sub>2</sub>O<sub>2</sub> (NM + H<sub>2</sub>O<sub>2</sub> vs. control or single HM,  $P < 0.01$ ), and HM-cultured astrocytes had a significantly lower BrdU-positive percentage (vs. NM + H<sub>2</sub>O<sub>2</sub>,  $P < 0.01$ ; Figure 5C,D). This showed that HM could inhibit the hypertrophy and proliferation of active astrocytes after H<sub>2</sub>O<sub>2</sub>-induced oxidative injury.

### The Functional Activation of Astrocytes Induced by Oxidative Injury was Mitigated by Hydrogen-rich Medium

Glial fibrillary acidic protein immunocytochemistry visualized the hypertrophy of reactive astrogliosis after oxidant injury and was able to reflect functional changes of astrogliosis. Fluorescence intensity differences showed that excessive expression of GFAP was significantly induced by H<sub>2</sub>O<sub>2</sub> (vs. control or single HM,  $P < 0.01$ ) and was notably weakened by HM (vs. NM + H<sub>2</sub>O<sub>2</sub>,  $P < 0.01$ ; Figure 5A, B). The astrogliosis led to abnormally increased secretion of proinflammatory cytokines IL-1 $\beta$ , IL-6, and TNF- $\alpha$  (vs. control or single HM,  $P < 0.01$ ), and these could be weakened by HM (vs. NM + H<sub>2</sub>O<sub>2</sub>,  $P < 0.01$ ; Figure 6). These results further demonstrated that the functional activation of astrocytes, due to H<sub>2</sub>O<sub>2</sub>-induced oxidative injury, was decreased by hydrogen-rich medium.

## Discussion

As a novel antioxidant, hydrogen selectively reacts with HO $\bullet$  and ONOO $^-$ , which are the major free radicals causing cell damage, without disturbing metabolic oxidation–reduction reactions; hence, it produces fewer side effects [10,12,13]. Dissolving hydrogen in liquid (normal saline or cell medium) not only makes it safer and more convenient for administration, but also means that a higher concentration can be achieved [10,11]. Hydrogen has been found to have protective effects on many vital organs after

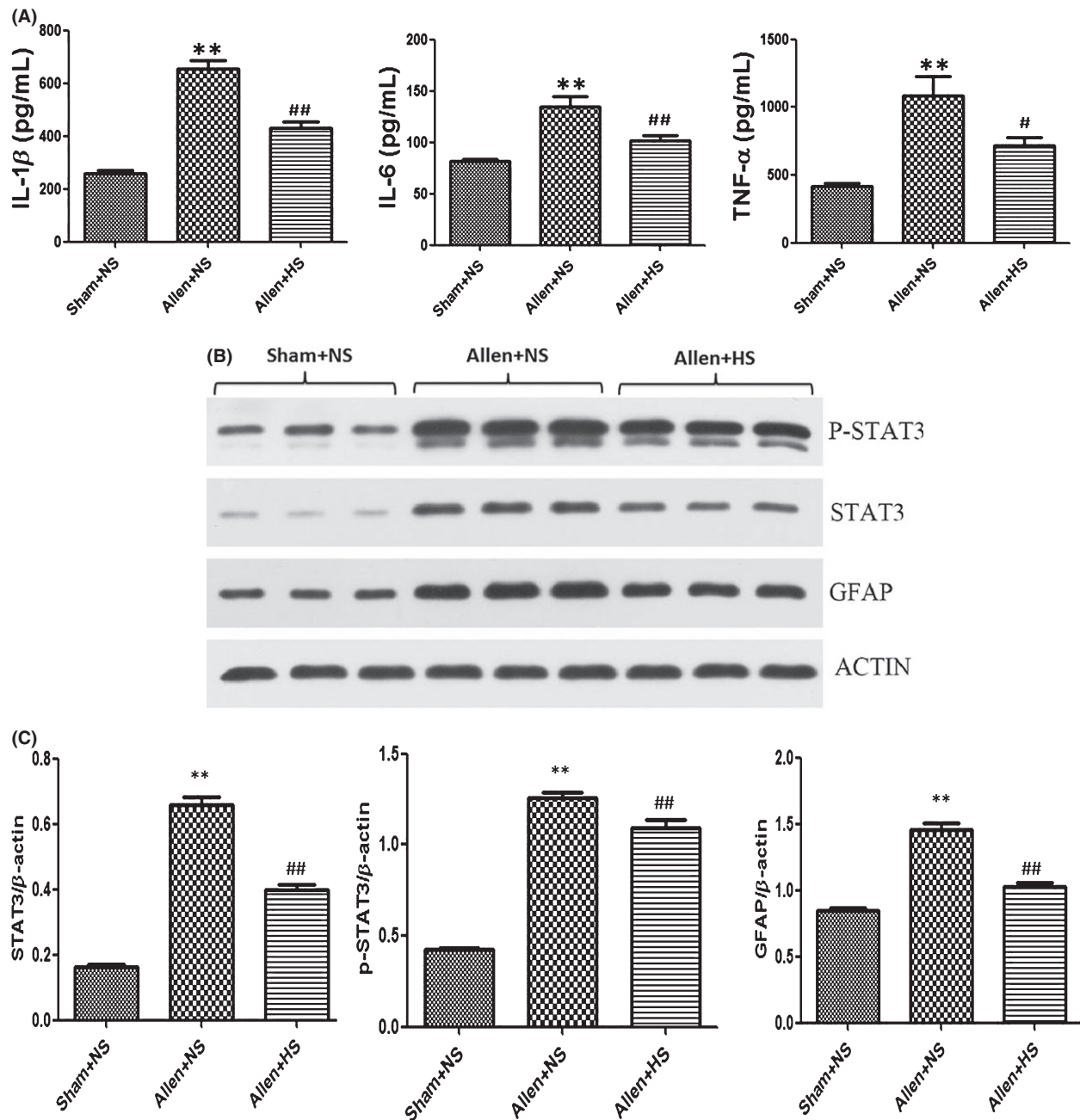


**Figure 1** On postoperation day (POD) 3, local contusive spinal cord segments were dissected for assay. The content of IL-1 $\beta$ , IL-6, and TNF- $\alpha$  was measured by ELISA, and the production of STAT3, p-STAT3, and glial fibrillary acidic protein (GFAP) expressed by astrocytes was assayed by Western blot. **(A)** Content of IL-1 $\beta$ , IL-6, and TNF- $\alpha$  (pg/mL) in each groups, respectively. **(B)** The expression of STAT3, p-STAT3, and GFAP. **(C)** Western blot data were expressed as gray values normalized to  $\beta$ -actin. The concentration of these proinflammatory cytokines was remarkably increased in the Allen + normal saline (NS) group and was notably attenuated by hydrogen-rich saline administration. The expression of these three proteins was increased in the NS group (vs. sham,  $P < 0.01$ ) and was significantly reduced by hydrogen-rich saline administrated intraperitoneally on POD 3 (vs. NS,  $P < 0.01$ ,  $P < 0.05$ , and  $P < 0.01$ , respectively). Results were means  $\pm$  SEM of three independent experiments. \*\* $P < 0.01$ , Allen + NS compared with sham; # $P < 0.05$  and ## $P < 0.01$ , Allen + hydrogen-rich saline compared with Allen + NS.

oxidative stress [10,11,14–16], but whether it can inhibit reactive astrogliosis and glial scar (an important factor of hindering nerve regeneration) after SCI has not been reported. In this study, we demonstrated that after SCI, hydrogen-rich liquid could suppress

the astrogliosis and subsequent glial scar and reduce the production of proinflammatory cytokines released by active astrocytes. Therefore, antiastrogliosis is a potential neuroprotective mechanism of molecular hydrogen.

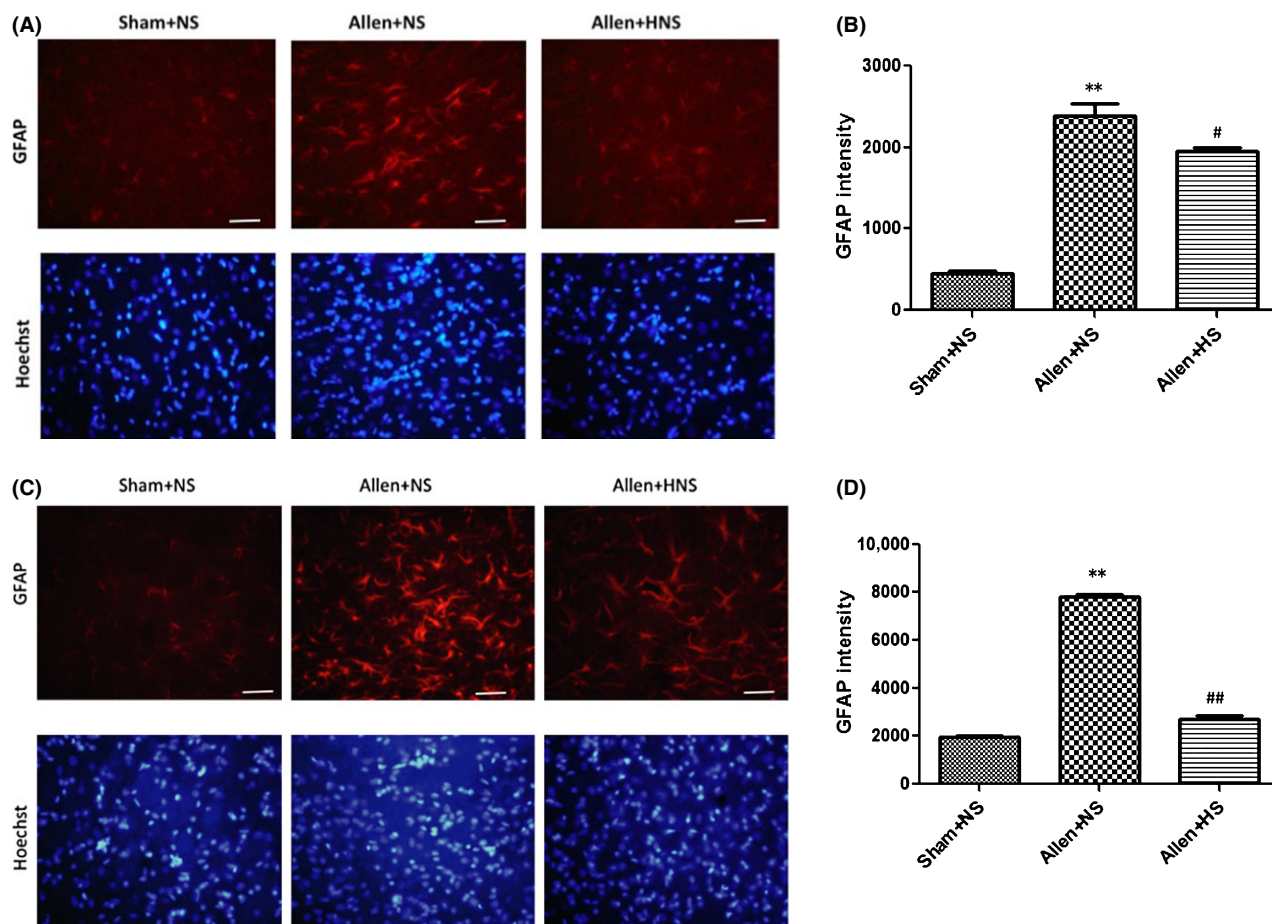


**Figure 2** (A, B) Immunohistochemistry of glial fibrillary acidic protein (GFAP) on postoperation day (POD) 7, and data were expressed with fluorescence intensity. (C) and (D) Immunohistochemistry of GFAP on POD 14, and its fluorescence intensity data. Morphologically, the characteristics of strongly activated astrocytes induced by contusive spinal cord injury were hypertrophy and hyperplasia, and the expression of GFAP (measured by the fluorescence intensity) was dramatically augmented on POD 7 and POD 14 (normal saline (NS) vs. sham,  $P < 0.01$ ). Hydrogen-rich saline administration significantly suppressed the reactive astroglialosis and alleviated the excessive expression of GFAP (vs. NS,  $P < 0.05$  and  $P < 0.01$ , respectively). Results were means  $\pm$  SEM of three independent experiments. \*\* $P < 0.01$ , Allen + NS vs. sham; # $P < 0.05$  and ## $P < 0.01$ , Allen + hydrogen-rich saline vs. Allen + NS. Scale bar = 100  $\mu$ m.

Reactive oxygen species is one of the major causes of astrocyte activation after SCI [5]. In the early stage, the activation of astrocytes has a defensive effect; however, as time progresses, excessive astroglialosis leads to pathologic changes impeding neural repair, such as producing neurotoxic levels of ROS, aggravating inflammation [8,21–24]. Moreover, active astrocytes can express inhibitory proteoglycan GFAP, which accumulates in the injury region, and form a glial scar, a crucial factor relating to poor clinical outcome [7,8,25]. In addition, the proinflammatory cytokines and ROS can exacerbate the scar formation through autocrine mechanisms [8]. Therefore, suppressing excessive astroglialosis to interrupt the vicious cycle is necessary and conducive to neuroprotection after SCI. We have shown that HS could decrease the content of lipid peroxidation and protein carbonyl after SCI [11]. Besides ROS, inflammatory factors primarily trigger astroglialosis in the acute period of SCI [8]. We found that HS could reduce the content of IL-1 $\beta$ , IL-6, and TNF- $\alpha$  in the spinal cord during the acute period (POD 3; HS vs. NS,  $P < 0.01$ ,  $P < 0.01$ , and  $P < 0.05$ ,

respectively; Figure 1A). This means that triggers of astroglialosis can be attenuated by HS. Astroglialosis and scar formation relate to several signaling pathways involving STAT3, JNK/c-Jun, TGF- $\beta$ /Smads, and so on [1,11,26–28]. STAT3 is the leading signaling pathway involved in astroglialosis [26,29]. Our results showed that on SCI POD 3, the expression of STAT3 and its functional formation, phosphorylated-STAT3 (p-STAT3), rose in the NS group (vs. sham,  $P < 0.01$ , both) and was distinctly downregulated by HS administration (vs. NS,  $P < 0.01$  and  $P < 0.05$ , respectively; Figure 1B,C). HS could inhibit the major signaling pathway of astroglialosis.

Glial fibrillary acidic protein belongs to intermediate filaments and is regarded as a sensitive and reliable indicator of astroglialosis after CNS injury [6,26,30]. On SCI POD 3, the expression of GFAP was obviously reduced by HS (vs. NS,  $P < 0.01$ ; Figure 1B,C), which was consistent with the changes of STAT3 and p-STAT3 signals. Morphologically, the characteristics of severe astroglialosis include obvious hypertrophy of the cell body and pronounced

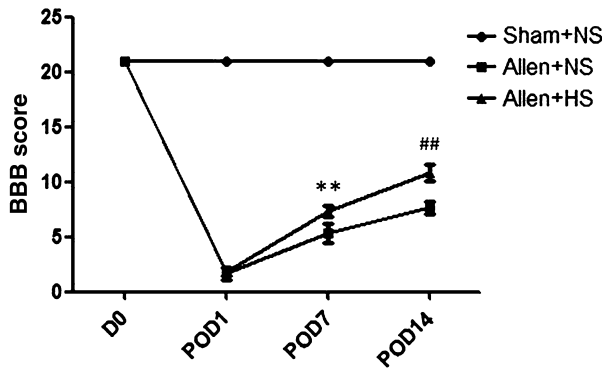


**Figure 3** Locomotor function was evaluated before surgery (D 0) and on postoperation days (PODs) 1, 7, and 14 using the Basso, Beattie, and Bresnahan locomotor scale (BBB scale). Spinal cord injury severely affected the locomotor function of animals (normal saline (NS) vs. sham,  $P < 0.01$ ). Rats in the hydrogen-rich saline (HS) group exhibited higher BBB scores on PODs 7 and 14 (vs. NS,  $P < 0.01$ ) and revealed a treatment effect of HS over time ( $P < 0.01$ ). Results were means  $\pm$  SEM of three independent experiments. \*\* $P < 0.01$  and ## $P < 0.01$ , Allen + HS vs. Allen + NS.

proliferation which overlaps, blurs, and disrupts neighboring astrocytes' domains [1]. The accumulation of the inhibitory extracellular matrix (EMC) gradually results in the formation of the

glial scar [31]. Whether the SCI is complete or not, neuronal plasticity will occur throughout the neuraxis, which is related to the synaptic rearrangements, the properties, changes of the spared neuronal circuitries, collateral sprouting, and so on [32]. Moreover, neuronal plasticity is the base mechanism of locomotor improvement [33,34]. Locomotor improvement after SCI depends on not only the intrinsic growth ability of the neurons but also the balance between growth inhibition and promotion from the extracellular matrix [32]. The glial scar has been regarded as a critical factor hindering axonal repair and regeneration [6–9]; therefore, it affects the neuronal plasticity and the locomotor improvement. The excessive expression of GFAP becomes much more prominent 7 days after CNS injury [31,35], so we also took PODs 7 and 14 as time points for investigating the extent of astrogliosis. Intraperitoneal injections of HS indeed suppressed astrogliosis and decreased GFAP expression after SCI (HS vs. NS,  $P < 0.05$  and  $P < 0.01$ , respectively; Figure 2). In particular, the astrogliosis was suppressed more significantly on POD 14, although it was slightly significant on POD 7 (65.7% vs. 18.2%,  $P < 0.01$ ). Meanwhile, we also demonstrated that intraperitoneal injections of HS could improve the hind limb locomotor function (HS vs. NS,  $P < 0.01$ ; Figure 3). These results support the idea that HS can relieve the barrier of glial scar, hence reduces the axonal injury and promotes the functional recovery. We purified primary astrocytes to eliminate the interference of other cells, such as microglia and

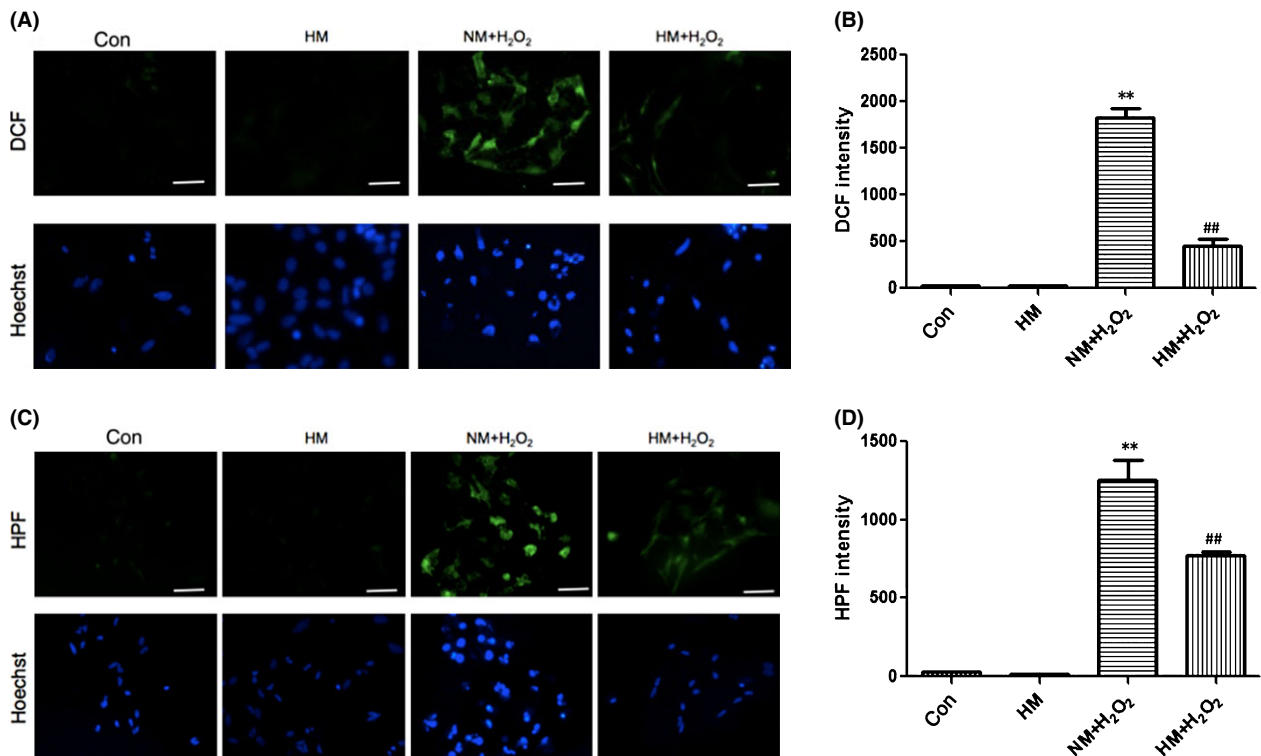


**Figure 4** Twelve hours after adding H<sub>2</sub>O<sub>2</sub> (100  $\mu$ M) and FeCl<sub>2</sub> (15  $\mu$ M) to the medium, with or without super-saturated hydrogen, intracellular reactive oxygen species (ROS) levels of each cultured astrocyte group were assayed. **(A)** and **(B)** Intracellular ROS levels were measured by the intensity of DCF. **(C)** and **(D)** Intracellular HO $\cdot$  levels were measured by the intensity of hydroxyphenyl fluorescein. There was no difference between control and single hydrogen-rich medium groups, but the total amounts of ROS and HO $\cdot$  were distinctly increased by H<sub>2</sub>O<sub>2</sub> (vs. control,  $P < 0.01$ ) and were notably decreased by hydrogen-rich medium (HM) treatment (vs. normal medium, NM + H<sub>2</sub>O<sub>2</sub>,  $P < 0.01$ ). Results were means  $\pm$  SEM of three independent experiments. \*\* $P < 0.01$ , NM + H<sub>2</sub>O<sub>2</sub> vs. control; ## $P < 0.01$ , H<sub>2</sub>O<sub>2</sub> + HM vs. H<sub>2</sub>O<sub>2</sub> + NM. Scale bar = 50  $\mu$ m.

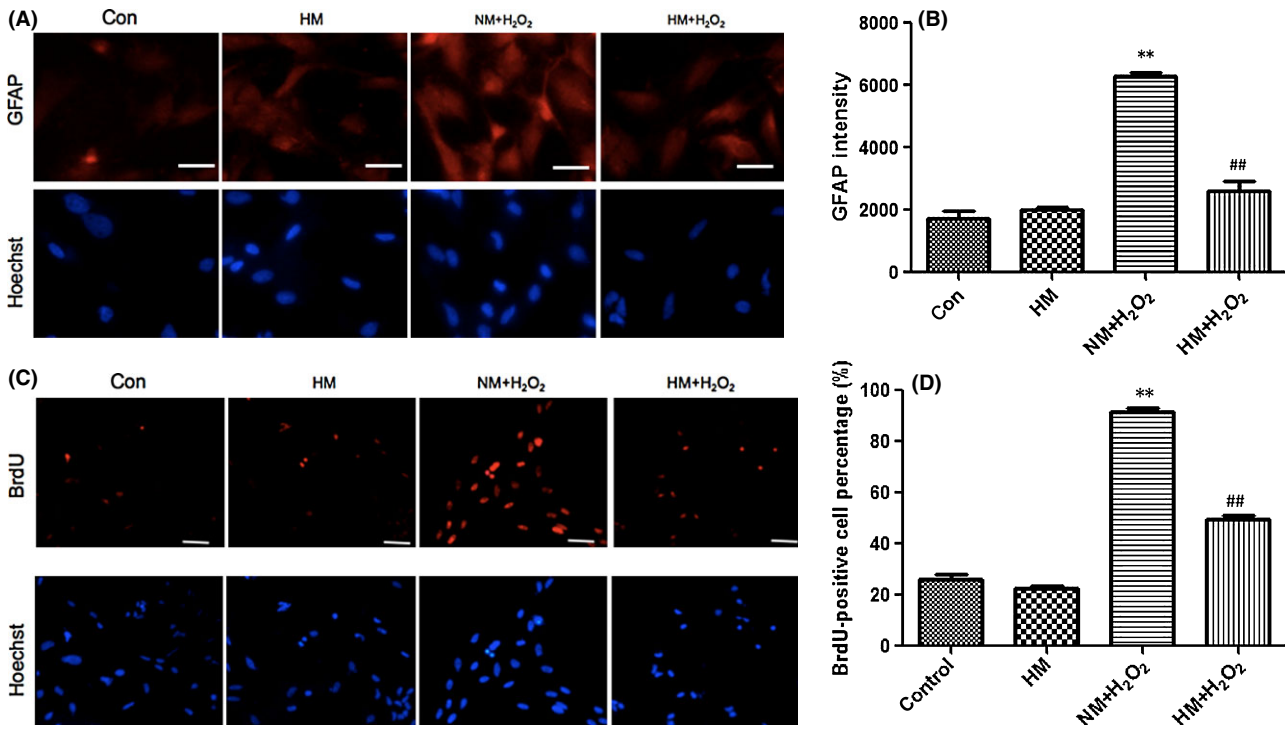


**Figure 5** Twelve hours after adding H<sub>2</sub>O<sub>2</sub> (100 μM) and FeCl<sub>2</sub> (15 μM) to the medium, with or without super-saturated hydrogen, the hypertrophy and proliferation of cultured astrocytes were observed. (A) and (B) Immunocytochemistry of glial fibrillary acidic protein (GFAP) demonstrating the morphological characteristics of hypertrophy and excessive expression of GFAP, and the fluorescence intensity data. (C) and (D) Images demonstrating the DNA synthesis of BrdU, which reflects the proliferation of astrocytes, and the percentage of positive cells. Hypertrophy, proliferation, and excessive expression of GFAP were obviously induced by H<sub>2</sub>O<sub>2</sub> in the normal medium (NM) + H<sub>2</sub>O<sub>2</sub> group (vs. control, *P* < 0.01) and were significantly inhibited by treatment with hydrogen-rich medium (vs. NM + H<sub>2</sub>O<sub>2</sub>, *P* < 0.01). Results were means ± SEM of three independent experiments. \*\**P* < 0.01, NM + H<sub>2</sub>O<sub>2</sub> vs. control; ##*P* < 0.01, H<sub>2</sub>O<sub>2</sub> + hydrogen-rich saline vs. H<sub>2</sub>O<sub>2</sub> + normal saline. Scale bar for A = 20 μm and for C = 50 μm.

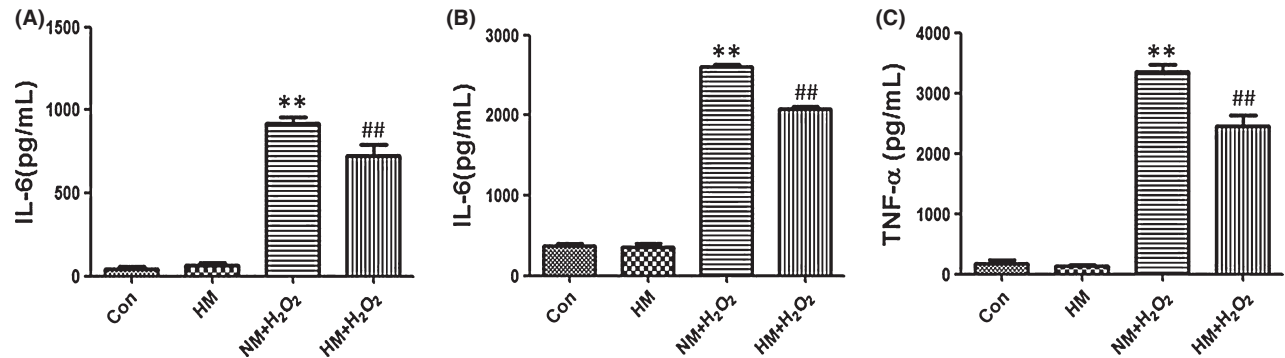


**Figure 6** Twelve hours after adding H<sub>2</sub>O<sub>2</sub> (100 μM) and FeCl<sub>2</sub> (15 μM) to the medium, with or without super-saturated hydrogen, the supernatant of each group was collected for ELISA to assay the secretion of proinflammatory cytokines by active, cultured astrocytes. (A) Content of IL-1β (pg/mL). (B) Content of IL-6 (pg/mL). (C) Content of TNF-α (pg/mL). H<sub>2</sub>O<sub>2</sub> led to the abnormally increased secretion of IL-1β, IL-6, and TNF-α (vs. control or single hydrogen-rich medium (HM), *P* < 0.01). Secretion of these cytokines could be reduced by hydrogen-rich medium (vs. NM + H<sub>2</sub>O<sub>2</sub>, *P* < 0.01). Results were means ± SEM of three independent experiments. \*\**P* < 0.01, NM + H<sub>2</sub>O<sub>2</sub> vs. control; ##*P* < 0.01, H<sub>2</sub>O<sub>2</sub> + hydrogen-rich saline vs. H<sub>2</sub>O<sub>2</sub> + normal saline.

macrophages, which can also secrete proinflammatory cytokines. The oxidative injury of astrocytes was induced by 100 μM H<sub>2</sub>O<sub>2</sub> and 15 μM FeCl<sub>2</sub>. Both intracellular H<sub>2</sub>O<sub>2</sub> and HO• result in detrimental effects and cell damage [36]. We demonstrated that 12 h after oxidative injury, HM reduced the intracellular synthesis of ROS and especially HO• (HM + H<sub>2</sub>O<sub>2</sub> vs. NM + H<sub>2</sub>O<sub>2</sub>, *P* < 0.01;

Figure 4). Hypertrophy and hyperplasia and functional changes also took place 12 h after H<sub>2</sub>O<sub>2</sub>-induced injury. The significant decrease in GFAP intensity and BrdU-positive cells supports the idea that HM could suppress astrogliosis (HM + H<sub>2</sub>O<sub>2</sub> vs. NM + H<sub>2</sub>O<sub>2</sub>, *P* < 0.01, both; Figure 5). Besides, the secretion of IL-1β, IL-6, and TNF-α, produced by astrocytes 12 h after



H<sub>2</sub>O<sub>2</sub>-induced injury, could also be reduced by HM (vs. NM + H<sub>2</sub>O<sub>2</sub>,  $P < 0.01$ ; Figure 6). The above results verified that molecular hydrogen could suppress the astrogliosis and related inflammation after SCI and oxidative injury. Antiastrogliosis may be a neuroprotective mechanism of molecular hydrogen.

Furthermore, excessive astrocyte activation may cause other detrimental effects that were not investigated in this study, involving damaging blood-brain barrier function by vascular endothelial growth factor (VEGF) production, releasing excitotoxic glutamate, inducing cytotoxic edema through AQP4 over activity, and contributing to chronic pain and seizures [1, 37–40]. Therefore, it is imperative to inhibit excessive reactive astrogliosis after SCI. Whether molecular hydrogen can improve these mentioned detrimental effects during CNS trauma and other related CNS diseases, such as neuropathic pain, neurodegenerative disease, and tumor, still requires further research.

In conclusion, administered in the form of hydrogen-rich liquid, molecular hydrogen could suppress reactive astrogliosis

after contusive SCI and reduce the release of proinflammatory cytokines produced by active astrocytes related to oxidative injury. Antiastrogliosis is a neuroprotective effect of molecular hydrogen, which supports its clinical application during SCI to promote neuroprotection, as well as functional restoration.

## Acknowledgments

This research was partly supported by the project from the Military Science Research of PLA (CWS11J121 to Dr. Yuan) and the Natural Science Foundation of China (81200953 to Dr. Xu).

## Conflict of Interest

We have not published or submitted the manuscript elsewhere simultaneously. The authors taking part in this study declared that they do not have any conflict of interests in this manuscript.

## References

- Sofroniew MV, Vinters HV. Astrocytes: Biology and pathology. *Acta Neuropathol* 2010;**119**:7–35.
- Bains M, Hall ED. Antioxidant therapies in traumatic brain and spinal cord injury. *Biochim Biophys Acta* 2012;**1822**:675–684.
- Xiong Y, Rabchevsky AG, Hall ED. Role of peroxynitrite in secondary oxidative damage after spinal cord injury. *J Neurochem* 2007;**100**:639–649.
- Yin X, Yin Y, Cao FL, et al. Tanshinone IIA attenuates the inflammatory response and apoptosis after traumatic injury of the spinal cord in adult rats. *PLoS ONE* 2012;**7**:e38381.
- Sofroniew MV. Molecular dissection of reactive astrogliosis and glial scar formation. *Trends Neurosci* 2009;**32**:638–647.
- Pekny M, Pekna M. Astrocyte intermediate filaments in CNS pathologies and regeneration. *J Pathol* 2004;**204**:428–437.
- Silver J, Miller JH. Regeneration beyond the glial scar. *Nat Rev Neurosci* 2004;**5**:146–156.
- Karimi-Abdolrezaee S, Billakanti R. Reactive astrogliosis after spinal cord injury-beneficial and detrimental effects. *Mol Neurobiol* 2012;**46**:251–264.
- Wu J, Pajoohesh-Ganji A, Stoica BA, Dinizo M, Guanciale K, Faden AI. Delayed expression of cell cycle proteins contributes to astroglial scar formation and chronic inflammation after rat spinal cord contusion. *J Neuroinflammation* 2012;**9**:169.
- Ohsawa I, Ishikawa M, Takahashi K, et al. Hydrogen acts as a therapeutic antioxidant by selectively reducing cytotoxic oxygen radicals. *Nat Med* 2007;**13**:688–694.
- Chen C, Chen Q, Mao Y, et al. Hydrogen-rich saline protects against spinal cord injury in rats. *Neurochem Res* 2010;**35**:1111–1118.
- James AM, Cocheme HM, Murphy MP. Mitochondria-targeted redox probes as tools in the study of oxidative damage and ageing. *Mech Ageing Dev* 2006;**126**:982–986.
- Sun H, Chen L, Zhou W, et al. The protective role of hydrogen-rich saline in experimental liver injury in mice. *J Hepatol* 2011;**54**:471–480.
- Liu Q, Shen WF, Sun HY, et al. Hydrogen-rich saline protects against liver injury in rats with obstructive jaundice. *Liver Int* 2010;**30**:958–968.
- Sun Q, Kang Z, Cai J, et al. Hydrogen-rich saline protects myocardium against ischemia-reperfusion injury in rats. *Exp Biol Med* 2009;**234**:1212–1219.
- Zheng X, Mao Y, Cai J, et al. Hydrogen-rich saline protects against intestinal ischemia/reperfusion injury in rats. *Free Radic Res* 2009;**43**:478–484.
- Tsai MJ, Liao JF, Lin DY, et al. Silymarin protects spinal cord and cortical cells against oxidative stress and lipopolysaccharide stimulation. *Neurochem Int* 2010;**57**:867–875.
- Gao XF, Wang W, Yu Q, Geoffrey B, Xiang ZH, He C. Astroglial P2X7 receptor current density increased following long-term exposure to rotenone. *Purinergic Signalling* 2011;**7**:65–72.
- Noda K, Tanaka Y, Shigemura N, et al. Hydrogen-supplemented drinking water protects cardiac allografts from inflammation-associated deterioration. *Transpl Int* 2012;**25**:1213–1222.
- Campbell AM, Zagon IS, McLaughlin PJ. Astrocyte proliferation is regulated by the OGF-OGFr axis in vitro and in experimental autoimmune encephalomyelitis. *Brain Res Bull* 2013;**90**:43–51.
- Hamby ME, Hewett JA, Hewett SJ. TGF-beta1 potentiates astrocytic nitric oxide production by expanding the population of astrocytes that express NOS-2. *Glia* 2006;**54**:566–577.
- Swanson RA, Ying W, Kauppinen TM. Astrocyte influences on ischemic neuronal death. *Curr Mol Med* 2004;**4**:193–205.
- Brambilla R, Bracchi-Ricard V, Hu WH, et al. Inhibition of astroglial nuclear factor kappaB reduces inflammation and improves functional recovery after spinal cord injury. *J Exp Med* 2005;**202**:145–156.
- Brambilla R, Persaud T, Hu X, et al. Transgenic inhibition of astroglial NF-kappaB improves functional outcome in experimental autoimmune encephalomyelitis by suppressing chronic central nervous system inflammation. *J Immunol* 2009;**182**:2628–2640.
- Busch SA, Silver J. The role of extracellular matrix in CNS regeneration. *Curr Opin Neurobiol* 2007;**17**:120–127.
- Herrmann JE, Imura T, Song B, et al. STAT3 is a critical regulator of astrogliosis and scar formation after spinal cord injury. *J Neurosci* 2008;**28**:7231–7243.
- Neary JT, Zimmermann H. Trophic functions of nucleotides in the central nervous system. *Trends Neurosci* 2009;**32**:189–198.
- Gadea A, Schinelli S, Gallo V. Endothelin-1 regulates astrocyte proliferation and reactive gliosis via a JNK/c-Jun signaling pathway. *J Neurosci* 2008;**28**:2394–2408.
- Kang W, Hébert JM. Signaling pathways in reactive astrocytes, a genetic perspective. *Mol Neurobiol* 2011;**43**:147–154.
- Pekny M, Leveen P, Pekna M, et al. Mice lacking glial fibrillary acidic protein display astrocytes devoid of intermediate filaments but develop and reproduce normally. *EMBO J* 1995;**14**:1590–1598.
- Gwak YS, Kang J, Unabia GC, Hulsebosch CE. Spatial and temporal activation of spinal glial cells: Role of gliopathy in central neuropathic pain following spinal cord injury in rats. *Exp Neurol* 2012;**234**:362–372.
- Onifer SM, Smith GM, Fouad K. Plasticity after spinal cord injury: Relevance to recovery and approaches to facilitate it. *Neurotherapeutics* 2011;**8**:283–293.
- Dietz V. Neuronal plasticity after a human spinal cord injury: Positive and negative effects. *Exp Neurol* 2012;**235**:110–115.
- Fouad K, Tse A. Adaptive changes in the injured spinal cord and their role in promoting functional recovery. *Neurol Res* 2008;**30**:17–27.
- Andrade MS, Hanania FR, Daci K, Leme RJ, Chadi G. Contuse lesion of the rat spinal cord of moderate intensity leads to a higher time-dependent secondary neurodegeneration than severe one. An open-window for experimental neuroprotective interventions. *Tissue Cell* 2008;**40**:143–156.
- Lee MN, Lee SH, Lee MY, et al. Effect of dihydrotestosterone on mouse embryonic stem cells exposed to H<sub>2</sub>O<sub>2</sub>-induced oxidative stress. *J Vet Sci* 2008;**9**:247–256.
- Takano T, Kang J, Jaiswal JK, et al. Receptor-mediated glutamate release from volume sensitive channels in astrocytes. *Proc Natl Acad Sci USA* 2005;**102**:16466–16471.
- Tian GF, Azmi H, Takano T, et al. An astrocytic basis of epilepsy. *Nat Med* 2005;**11**:973–981.
- Argaw AT, Guriein BT, Zhang Y, Zameer A, John GR. VEGF-mediated disruption of endothelial CLN-5 promotes blood-brain barrier breakdown. *Proc Natl Acad Sci USA* 2009;**106**:1977–1982.
- Milligan ED, Watkins LR. Pathological and protective roles of glia in chronic pain. *Nat Rev Neurosci* 2009;**10**:23–36.